Event-Triggered Dynamic State Estimation in Power Systems Using a Data-Selective Set-Membership Filter

R. BORAGOLLA, P. YAHAMPATH, U. ANNAKKAGE
University of Manitoba
Canada

SUMMARY

In future deregulated power grids, dynamic state estimation (DSE) enabled by phasor measurement units (PMUs) and data networks will play an important role in system monitoring operations [1]. While the high sampling rates of PMUs will enable monitoring at unprecedented accuracies, high data rates will impose a heavy burden on data networks. Multi-area state estimation (MASE), where a large power grid is divided into sectors and local state estimates of each sector are communicated to a monitoring center for further processing is a potential solution. The true benefit of MASE can however be realized by using local estimators capable of sending their estimates to the monitoring center only during periods of significant events. This will necessitate new event-triggered state estimators, as opposed to continuous estimators such as the conventional Kalman filter (KF). [2].

We investigate the applicability of a class of DSE algorithms known as set-membership filters (SMFs) which inherently posses a so called data-selective property [3] that can be exploited in event-triggered state estimation. Similar to the KF, an SMF also relies on time iterations of prediction and correction steps. However, unlike the KF, an SMF can be easily designed to perform the measurement-driven correction steps only when the observed measurements are sufficiently informative (data-selective). In a typical power system, an SMF will therefore perform only prediction steps much of the time, with correction steps coming into effect only during a system abnormality such as a fault condition. Since the prediction step alone can be carried out at the remote monitoring center as well, the local SMFs need to send the information required for the correction steps only during fault conditions. The basic principle behind an SMF is to use bounding sets for random variables rather than probability distributions. In this paper, we will describe a computationally simple linear SMF algorithm for DSE, which is based on ellipsoidal bounding sets, including the computations required for the prediction step and the data-selective correction step. We will also present an extension to non-linear DSE, based on locally linear approximations.

We then present an experimental study aimed at evaluating the suitability of the SMF algorithm for evened-triggered DSE. In this study, we consider the simulation of a six-state system consisting of a single machine infinite bus system (SMIB) with a synchronous generator [4]. The SMF algorithm is used to track the synchronous generator states under steady-state conditions as well as under disturbances caused by fault conditions, which allows us to observe the ability of the SMF algorithm to track the state under steady-state conditions without requiring any correction-step updates (thus, for example, ignoring PMU measurements), while maintaining accurate tracking during a fault using frequent correction steps. Simulation results are presented which demonstrate that (1) in terms of accuracy, the data-selective SMF
borbnwmr@myumanitoba.ca.

performs identically to the continually updating extended KF, and (2) the SMF only performs the correction step less than 50% of the time during transient and disturbances. The impact of inevitable modeling errors on the performance of the SMF is also investigated.

KEYWORDS

1 INTRODUCTION

Power system state estimation (PSSE) is a powerful tool for monitoring and control of a power grid [5,6]. Traditionally, PSSE has relied on supervisory control and data acquisition (SCADA) measurements, typically updated at 2-4 second intervals. Such low measurement rates permit only static-state estimation which has a limited usefulness in real-time monitoring. The recent introduction of synchronized phasor measurement units (PMUs) which can directly record measurements, at rates as high as 120 frames per second [7], presents new opportunities for real-time power system monitoring through dynamic state estimation (DSE) [2]. Nevertheless, the large amounts of data produced by PMU networks will necessitate multi-area state estimation (MASE) [8] to ease the burden on communication infrastructure. In MASE, many distributed local state estimators are employed which communicate their estimates to a centralized monitoring center for fusion. To reduce the communication overhead, PMU-based MASE will require new event-triggered or data-selective state estimators. A class of algorithms that inherently possesses the data-selective estimation capability is set membership filters (SMFs) [9–14].

An SMF is also based on the familiar prediction-correction recursive structure of the statistical state estimation algorithms such as the Kalman filter (KF) [15]. However, in contrast to KF, SMF can be designed to produce a new state estimate only when the observations contain significant innovation. Unlike statistical approaches that assume probability distributions for the random variable (for example in the KF, those are assumed to be jointly Gaussian), an SMF only assumes the uncertainties associated with those belong to bounded sets in Euclidean space, referred to as membership sets or bounding sets. Typically noise variables are assumed to have known membership sets which are chosen based on prior knowledge about the bounds of these variables. Given the membership set for the state vector found at a time instant $k-1$, the SMF will determine a new membership set for the state vector at time k which is consistent with the given state-space model, assumed membership sets, and the current observation vector. The estimation error at any time step will be represented by its membership set.

An important feature of the SMF formulation is the possibility of a data-selective correction step that can be skipped by checking a condition. More specifically, if the size of the membership set for the state vector obtained in the prediction step can not be further decreased by a correction based on the given observation vector the update-step is skipped. An SMF estimator only determines a most likely membership set for the state vector. If a point estimate is desired, a suitable value within the membership set can be chosen. Furthermore, in applications where reliability and safety are the concerns, an acceptable bound on the state, rather than a point estimate may be all that is required [11].

While SMF is not widely known in the PSSE community, this approach has been considered for various purposes previously. Application of SMF in state estimation [9–12, 14], and parameter estimation [16] can be found in the context of controls and adaptive signal processing. The main goal of this paper is to bring to light the potential applicability of the ellipsoidal SMF (E-SMF) for event-triggered DSE. Ellipsoidal bounding sets are most common in SMF due to its advantages over other bounding sets such as hypercubes, polytopes, intervals, etc. [17]. This is mainly due to the fact that they lead to simpler mathematical formulations. First, we present basic principles of ellipsoidal SMF for state estimation in linear systems and an extension to non-linear systems based on locally linear approximations. Then the feasibility of applying SMF in the context of power system is studied using a six state system consisting of single machine infinite bus system (SMIB) with synchronous generator. It has been observed in this study, that the data-selective SMF performs identical to the extended KF (EKF) in terms of accuracy, but only performs the correction step less than 50% of the time during a disturbance. Finally, the impact of inevitable modeling errors on the performance of the SMF is also investigated.

Preliminaries :

An ellipsoidal set $\mathbb{E} \subset \mathbb{R}^N$ with the center $\boldsymbol{c} \in \mathbb{R}^N$ can be defined by two equivalent forms

$$\mathbb{E}(\boldsymbol{c}, \boldsymbol{P}, \sigma^2) = \{\boldsymbol{c} \in \mathbb{R}^n : (\boldsymbol{x} - \boldsymbol{c})^T \boldsymbol{P}^{-1} (\boldsymbol{x} - \boldsymbol{c}) \leq \sigma^2\}, \tag{1}$$

$$= \{\boldsymbol{c} \in \mathbb{R}^n : (\boldsymbol{x} - \boldsymbol{c})^T \sigma^2 \boldsymbol{P}^{-1} (\boldsymbol{x} - \boldsymbol{c}) \leq 1\},$$

where $\boldsymbol{P} \in \mathbb{R}^{N \times N}$ is a symmetric positive semi-definite matrix that defines the shape of the ellipsoid (shape-matrix) and σ^2 is a scaling factor.

2 DATA SELECTIVE SMF STATE ESTIMATOR

In this section, we describe the SMF algorithm used in our study which is based on [3, 18, 19]. We first consider the state estimation in a linear dynamical system. As outlined at the end of this section, the solution can be easily extended to a nonlinear system by using the method of local linearization as in the case of EKF [20].

2.1 E-SMF algorithm for linear systems

Consider the discrete-time linear dynamical system given by the general state-space model,

$$\boldsymbol{x}_k = \boldsymbol{A}_k \boldsymbol{x}_{k-1} + \boldsymbol{w}_k, \tag{2}$$

$$\boldsymbol{y}_k = \boldsymbol{C}_k \boldsymbol{x}_k + \boldsymbol{v}_k, \tag{3}$$

where k is discrete time index, $\boldsymbol{x}_k \in \mathbb{R}^n$ is the state vector, $\boldsymbol{y}_k \in \mathbb{R}^m$ is the observation vector (n is the number of states and m is the number of measurements), and $\boldsymbol{w}_k \in \mathbb{R}^n$ and $\boldsymbol{v}_k \in \mathbb{R}^m$ are random noise vectors. The state transition matrix $\boldsymbol{A}_k \in \mathbb{R}^{n \times n}$ and the observation matrix $\boldsymbol{C}_k \in \mathbb{R}^{m \times n}$ are assumed to be known. E-SMF algorithm treats a random vector as an unknown vector with an ellipsoidal membership set (EMS). The EMSs of the noise vector $\boldsymbol{w}_k$ and $\boldsymbol{v}_k$ are assumed a prior known. Let these be given by $\mathbb{E}(\boldsymbol{0}, \boldsymbol{W}_k, 1)$ and $\mathbb{E}(\boldsymbol{0}, \boldsymbol{V}_k, 1)$ respectively. It is assumed that noise is zero mean.

The basis of the E-SMF algorithm is that, given an EMS for the initial system state $\boldsymbol{x}_0$, use (2) and (3) to recursively compute an updated EMS for $\boldsymbol{x}_k$ for $k = 1, 2, ...$, based on the observation $\boldsymbol{y}_k$ and the EMS computed at time $k-1$. More specifically let $\mathbb{E}(\boldsymbol{x}_{k-1}, \boldsymbol{P}_{k-1}, \sigma_{k-1}^2)$ be the EMS obtained for $\boldsymbol{x}_{k-1}$ after observing $\boldsymbol{y}_1, ..., \boldsymbol{y}_{k-1}$. Then, in prediction step at time k, we obtain a predicted EMS for $\boldsymbol{x}_{k|k-1}$ using the state-transition equation (2), and by taking the vector sum of $\mathbb{E}(\boldsymbol{x}_{k-1}, \boldsymbol{P}_{k-1}, \sigma_{k-1}^2)$ projected in time and $\mathbb{E}(\boldsymbol{0}, \boldsymbol{W}_k, 1)$, $\mathbb{T}_k = \boldsymbol{A}_k \mathbb{E}(\boldsymbol{x}_{k-1}, \boldsymbol{P}_{k-1}, \sigma_{k-1}^2) \oplus \mathbb{E}(\boldsymbol{0}, \boldsymbol{W}_k, 1)$. The resulting set is not necessarily ellipsoidal. Let $\mathbb{E}(\boldsymbol{x}_{k|k-1}, \boldsymbol{P}_{k|k-1}, \sigma_{k|k-1}^2)$ be the predicted EMS for $\boldsymbol{x}_{k|k-1}$. Next, the correction step for time k uses the new observation $\boldsymbol{y}_k$ and the observation equation (3) to correct the predicted EMS and obtains an updated EMS $\mathbb{E}(\boldsymbol{x}_k, \boldsymbol{P}_k, \sigma_k^2)$ for $\boldsymbol{x}_k$. The exact membership set for $\boldsymbol{x}_k$ is the intersection of two ellipsoidal sets $\mathbb{E}(\boldsymbol{x}_{k|k-1}, \boldsymbol{P}_{k|k-1}, \sigma_{k|k-1}^2)$ and $\mathbb{S}_k = \{\boldsymbol{x} \in \mathbb{R}^n : (\boldsymbol{y}_k - \boldsymbol{C}_k \boldsymbol{x})^T \boldsymbol{V}_k^{-1} (\boldsymbol{y}_k - \boldsymbol{C}_k \boldsymbol{x}) \leq 1\}$ the result of which is not necessarily ellipsoidal either.

In both prediction and correction steps ellipsoidal sets will be fitted to non-ellipsoidal sets $\mathbb{T}_k$ and $\mathbb{E}(\boldsymbol{x}_{k|k-1}, \boldsymbol{P}_{k|k-1}, \sigma_{k|k-1}^2) \cap \mathbb{S}_k$ in some optimal fashion. By minimizing the size of EMS we can find an optimal ellipsoid. The most common measures of the size of an ellipsoidal set are the geometric volume, or equivalently the determinant of the matrix $\sigma^2 \boldsymbol{P}$ (1) (determinant criterion), and the trace of $\sigma^2 \boldsymbol{P}$ (trace criterion) [17]. Note that E-SMF algorithm only finds an EMS for the state to be estimated. If required, the center of the EMS can be used as a single point estimate. The prediction and correction step calculations are as follows.

2.1.1 Prediction step

An ellipsoid which is a tight outer-bound to the vector sum $\mathbb{T}_k$ can be determined using trace minimization. In particular, from [17, Theorem 4.4] it follows that an ellipsoidal outer bound to $\mathbb{T}_k$ can be given by $\mathbb{E}(\boldsymbol{x}_{k|k-1}, \boldsymbol{P}_{k|k-1}, \sigma_{k|k-1}^2)$, where

$$\hat{\boldsymbol{x}}_{k|k-1} = \boldsymbol{A}_{k-1} \hat{\boldsymbol{x}}_{k-1},$$

$$\boldsymbol{P}_{k|k-1} = (1 - p_k)^{-1} \boldsymbol{A}_{k-1} \boldsymbol{P}_{k-1} \boldsymbol{A}_{k-1}^T + (\sigma_{k-1}^2 p_k)^{-1} \boldsymbol{W}_k, \tag{4}$$

$$\sigma_{k|k-1}^2 = \sigma_{k-1}^2, \tag{5}$$

and $p_k = \sqrt{\text{Tr}(\boldsymbol{W}_k)} \left(\sqrt{\sigma_{k|k-1}^2 \text{Tr}(\boldsymbol{A}_{k-1} \boldsymbol{P}_{k-1} \boldsymbol{A}_{k-1}^T)} + \sqrt{\text{Tr}(\boldsymbol{W}_k)} \right)^{-1}$. $\text{Tr}(\boldsymbol{M})$ denotes the trace of matrix $\boldsymbol{M}$.

2.1.2 Correction step

Let $\bar{V}_k$ be the lower triangular matrix obtained by Cholesky factorization $V_k^{-1} = \bar{V}_k \bar{V}_k^T$. Then, the set $\mathbb{S}_k$ can be expressed as $\mathbb{S}_k = \{x \in \mathbb{R}^n : \|\bar{y}_k - \bar{C}_k x\|^2 \le 1\}$, where $\bar{y}_k = \bar{V}_k^T y_k$ and $\bar{C}_k = \bar{V}_k^T C_k$. It can be shown that (see [3] and references therein) a class of ellipsoids parameterized by $0 \le \lambda_k \le 1$, that outer-bounds the intersection $\mathbb{E}(\hat{x}_{k|k-1}, P_{k|k-1}, \sigma^2_{k|k-1}) \cap \mathbb{S}_k$ is given by $E(\hat{x}_k, P_k, \sigma^2_k)$, where

$$\hat{x}_k = \hat{x}_{k|k-1} + \lambda_k P_{k|k-1} \bar{C}_k^T \delta_k,$$

$$P_k = \frac{1}{1 - \lambda_k}(I - \lambda_k P_{k|k-1} \bar{C}_k^T Q_k^{-1} \bar{C}_k)P_{k|k-1},$$

$$\sigma^2_k = (1 - \lambda_k)\sigma^2_{k|k-1} + \lambda_k - \lambda_k(1 - \lambda_k)\delta_k^T Q_k^{-1} \delta_k,$$

and we have defined $\delta_k = \bar{y}_k - \bar{C}_k \hat{x}_{k|k-1}$, $G_k = \bar{C}_k P_{k|k-1} \bar{C}_k^T$, and $Q_k = (1 - \lambda_k)I + \lambda_k G_k$. Note that δ_k can be considered as a prediction error. It is not simple to determine λ_k using determinant or trace criteria. Following [3, Theorem 2] we can find λ_k such that an upper bound to the determinant or the trace is minimized. The corresponding λ_k value is given by

$$\lambda_k^* = \begin{cases} 0 & \text{if } \|\delta_k\|^2 \le 1 - \sigma^2_{k|k-1} \\ \frac{1}{2}(1 - \beta_k) & \text{if } \bar{g}_k = 1 \\ \frac{1}{1 - \bar{g}_k}\left[1 - \sqrt{\frac{\bar{g}_k}{\nu_k}}\right] & \text{if } \nu_k > 0 \end{cases}$$

where $\bar{g}_k$ is the norm or the maximum eigenvalue of G_k, and we have defined $\nu_k = 1 + \beta_k(1 - \bar{g}_k)$ and $\beta_k = (1 - \sigma^2_{k|k-1})(\delta_k^T \delta_k)^{-1}$. Clearly if $\lambda_k = 0$, $\sigma^2_k P_k = \sigma^2_{k|k-1} P_{k|k-1}$, and the correction step will not change the ellipsoidal set for x_k, already obtained in the prediction step. The interpretation is that the observation y_k in this case does not contain sufficient innovation to refine the predicted EMS. This is the data-selective property of the correction step.

2.2 Extension to nonlinear systems

Consider the nonlinear dynamical system given by the general state-space model,

$$x_k = f(x_{k-1}) + w_k', \tag{6}$$

$$y_k' = h(x_k) + v_k', \tag{7}$$

where both f and h are assumed to be differentiable nonlinear functions with continuous first derivatives.
Prediction Step :
As before, let the EMS for the state vector computed at time $k - 1$ be $\mathbb{E}(\hat{x}_{k-1}, P_{k-1}, \sigma^2_{k-1})$. The Taylor series expansion of $f(x_{k-1})$ about the center $\hat{x}_{k-1}$ of this EMS is given by

$$f(x_{k-1}) = f(\hat{x}_{k-1}) + F(\hat{x}_{k-1})e_{k-1} + \varepsilon_f(e_{k-1}), \tag{8}$$

where $e_{k-1} = x_{k-1} - \hat{x}_{k-1}$, $F(x) = \dfrac{\partial f(x)}{\partial x}$ and $\varepsilon_f(e_{k-1})$ denotes the terms involving the higher order derivatives. Plugging (8) into (6) we obtain a state equation, linearized about the center of the ellipsoid $\mathbb{E}(\hat{x}_{k-1}, P_{k-1}, \sigma^2_{k-1})$, given by

$$x_k = A_{k-1}(x_{k-1} - \hat{x}_{k-1}) + f(\hat{x}_{k-1}) + w_k, \tag{9}$$

where we have defined $A_{k-1} = F(\hat{x}_{k-1})$ and $w_k = w_k' + \varepsilon_f(e_{k-1})$ is the effective noise vector which also includes the error resulting from linearization. Let $\mathbb{E}(0, W_k, 1)$ be the EMS for w_k. We now note that, given the EMS for x_{k-1} whose center is $\hat{x}_{k-1}$, (9) can be used to find a prediction for the membership set for x_k. This is the vector sum of two sets, given by $\mathbb{T}_k' = \mathbb{U}_k \oplus \mathbb{E}(0, W_k, 1)$, where $\mathbb{U}_k$ is the elliposidal

set obtained by translating the origin-centered ellipsoidal set $\boldsymbol{A}_{k-1}\mathbb{E}(\boldsymbol{0}, \boldsymbol{P}_{k-1}, \sigma_{k-1}^2)$ to the center $f(\hat{\boldsymbol{x}}_{k-1})$. While $\mathbb{T}'_k$ itself is not ellipsoidal, using the results from the Section 2.1.1, it is straightforward to verify that an ellipsoidal outer bound for $\mathbb{T}'_k$ is $\mathbb{E}(\hat{\boldsymbol{x}}_{k|k-1}, \boldsymbol{P}_{k|k-1}, \sigma_{k|k-1}^2)$ with $\hat{\boldsymbol{x}}_{k|k-1} = f(\hat{\boldsymbol{x}}_{k-1})$, is given by (4) and (5) respectively. Note that, in this case the shape matrix $\boldsymbol{W}_k$ of the noise vector $\boldsymbol{w}_k$ must be determined by using suitable bounds for $\boldsymbol{w}'_k$ in (6) as well as $\varepsilon_f(\boldsymbol{e}_{k-1})$.

Correction Step :

Using arguments similar to those in the previous section, we can linearize (7) about the center of the predicted EMS $\mathbb{E}(\hat{\boldsymbol{x}}_{k|k-1}, \boldsymbol{P}_{k|k-1}, \sigma_{k|k-1}^2)$ to obtain

$$\boldsymbol{y}'_k = \boldsymbol{C}_k(\boldsymbol{x}_k - \hat{\boldsymbol{x}}_{k|k-1}) + h(\hat{\boldsymbol{x}}_{k|k-1}) + \boldsymbol{v}_k, \tag{10}$$

where we define $\boldsymbol{C}_k = \left.\dfrac{\partial h(\boldsymbol{x})}{\partial \boldsymbol{x}}\right|_{\boldsymbol{x}=\hat{\boldsymbol{x}}_{k|k-1}}$ and $\boldsymbol{v}_k$ is the effective noise vector which also includes the linearization error. Now, by defining $\boldsymbol{y}_k = \boldsymbol{y}'_k + \boldsymbol{C}_k\hat{\boldsymbol{x}}_{k|k-1} - h(\hat{\boldsymbol{x}}_{k|k-1})$, we can convert (10) into the same form as (3). Thus, the correction step in this case can also be performed exactly as in Sec. 2.1.2.

3   SIMULATION RESULTS AND DISCUSSION

In this section, we investigate the performance of the E-SMF state estimator described in Sec. 2 through simulations. The example considered here is a SMIB system based on the system in [4, Fig. 5.2], which is shown in Fig. 1. As the generator G, we have used the constant flux linkage model for a
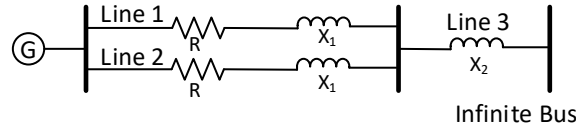

Figure 1: Experimental test set-up- SMIB system.

synchronous generator which includes the effects of the sub-transient circuit with one d-axis and two q-axis amortisseurs. The first order non-linear differential equations describing this model in dq frame are given by [4, 13.22-13.31]. After converting these continuous time equations to discrete-time, we can obtain the state space model given by (11) and (12). In these equations, δ is the rotor angle, $\Delta\omega$ is the rotor speed variation in per unit, $\omega_0 = 2\pi f_0$ where $f_0 = 60$ Hz is the base angular frequency, ψ_{fd} is the flux linkage in field winding, ψ_{1d} is the flux linkage in d-axis 1st amortisseur winding, ψ_{1q} is the flux linkage in q-axis 1st amortisseur winding, ψ_{2q} is the flux linkage in q-axis 2nd amortisseur winding, T_e is the real power output of the machine, E_{fd} is the field voltage supplied to the machine, T_m is the mechanical torque input to the machine, $H = 3.5000$ MWs/MVA is the inertia constant, and $D = 5$ is the damping factor. The other variables are defined in table 1, and we have defined

$$T_e = e_d i_d + e_q i_q, \qquad e_d = E_R\sin(\delta) - E_I\cos(\delta), \qquad e_q = E_I\sin(\delta) + E_R\cos(\delta),$$

$$e_{fd} = \frac{E_{fd}R_{fd}}{X_{ad}}, \qquad i_d = \frac{X''_{ad}}{X''_d}\left(\frac{\psi_{fd}}{X_{fd}} + \frac{\psi_{1d}}{X_{1d}}\right) - \frac{e_q}{X''_d}, \qquad i_q = \frac{X''_{aq}}{X''_q}\left(\frac{\psi_{1q}}{X_{1q}} + \frac{\psi_{2q}}{X_{2q}}\right) + \frac{e_d}{X''_q}.$$

Note that E_R and E_I are the real and imaginary components of the terminal voltage and calculated with respect to the common reference frame. The inputs to the state estimator are E_{fd}, T_m, E_I and E_R.

3.1   Numerical Results

The performance of the state estimator is measured by the time-averaged mean square error (MSE) given by

$$e_{\boldsymbol{x}_k} = \frac{1}{K}\sum_{k=1}^{K} E(x_{i,k} - \hat{x}_{i,k})^2, \quad i = 1, \ldots, n$$

6

$$\begin{pmatrix} \delta_k \\ \Delta\omega_k \\ \psi_{fd_k} \\ \psi_{1d_k} \\ \psi_{1q_k} \\ \psi_{2q_k} \end{pmatrix} = \begin{pmatrix} \delta_{k-1} + \Delta t \cdot \omega_0 \Delta\omega_{k-1} \\ \Delta\omega_{k-1} + \dfrac{\Delta t}{2H}\left(T_m + T_{ek-1} - D\Delta\omega_{k-1}\right) \\ \psi_{fd_{k-1}} + \Delta t \cdot \omega_0 \left[\dfrac{E_{fd}R_{fd}}{X_{ad}} - \dfrac{R_{fd}\psi_{fd_{k-1}}}{X_{fd}} + \dfrac{R_{fd}X_{ad}''}{X_{fd}}\left(-i_{dk-1} + \dfrac{\psi_{fd_{k-1}}}{X_{fd}} + \dfrac{\psi_{1d_{k-1}}}{X_{1d}}\right)\right] \\ \psi_{1d_{k-1}} + \Delta t \cdot \omega_0 \left[-\dfrac{R_{1d}\psi_{1d_{k-1}}}{X_{1d}} + \dfrac{R_{1d}X_{ad}''}{X_{1d}}\left(-i_{dk-1} + \dfrac{\psi_{fd_{k-1}}}{X_{fd}} + \dfrac{\psi_{1d_{k-1}}}{X_{1d}}\right)\right] \\ \psi_{1q_{k-1}} + \Delta t \cdot \omega_0 \left[-\dfrac{R_{1q}\psi_{1q_{k-1}}}{X_{1q}} + \dfrac{R_{1q}X_{aq}''}{X_{1q}}\left(-i_{qk-1} + \dfrac{\psi_{1q_{k-1}}}{X_{1q}} + \dfrac{\psi_{2q_{k-1}}}{X_{2q}}\right)\right] \\ \psi_{2q_{k-1}} + \Delta t \cdot \omega_0 \left[-\dfrac{R_{2q}\psi_{2q_{k-1}}}{X_{2q}} + \dfrac{R_{2q}L_{aq}''}{X_{2q}}\left(-i_{qk-1} + \dfrac{\psi_{1q_{k-1}}}{X_{1q}} + \dfrac{\psi_{2q_{k-1}}}{X_{2q}}\right)\right] \end{pmatrix} + \boldsymbol{w}_k' \tag{11}$$

$$\boldsymbol{y}_k = \begin{pmatrix} \hat{T}_{ek} \\ (\hat{\Delta\omega}_k + 1)\omega_0 \end{pmatrix} + \boldsymbol{v}_k' \tag{12}$$

Table 1: Generator data and line data.

Symbol	Definition	Value (per unit)
R_a	Stator resistance	0.0030
X_l	Stator leakage reactance	0.1500
X_d	D-axis unsaturated synchronous reactance	1.8098
X_q	Q-axis unsaturated synchronous reactance	1.7599
X_d''	D-axis unsaturated sub-transient reactance	0.2296
X_q''	Q-axis unsaturated sub-transient reactance	0.2500
X_{fd}	Field leakage reactance	0.1634
X_{1d}	D-axis 1st damper leakage reactance	0.1713
X_{1q}	Q-axis 1st damper leakage reactance	0.7252
X_{2q}	Q-axis 2st damper leakage reactance	0.1250
R_{fd}	Field resistance	0.00059938
R_{1d}	D-axis 1st damper resistance	0.0284
R_{1q}	Q-axis 1st damper resistance	0.0062
R_{2q}	Q-axis 2st damper resistance	0.0237
R	Line 1, 2 resistance	0.1250
X_1	Line 1, 2 reactance	0.6250
X_2	Line 3 reactance	0.1250

where $E(\cdot)$ is the statistical expectation operator, $\boldsymbol{x}_k = (x_{1,k}\dots x_{n,k})^T$ is the state vector, $\hat{\boldsymbol{x}}_k = (\hat{x}_{1,k}\dots\hat{x}_{n,k})^T$ is the estimate, and K is the duration of a simulation run in time steps. In obtaining the experimental results presented below, the statistical expectations have been estimated with Monte-Carlo trials over 100 different realizations of noise vectors.

It has been assumed that both $\boldsymbol{w}_k = (w_{1,k},\dots,w_{6,k})^T$ and $\boldsymbol{v}_k = (v_{1,k},v_{2,k})^T$ are uniformly distributed vectors, where $w_{i,k} \in [-10^{-5},10^{-5}]$ for $i = 1,\dots,6$, $v_{1,k} \in [-0.005,0.005]$, and $v_{2,k} \in [-0.05,0.05]$. The values for the $\boldsymbol{w}_k$ intervals are found by trial and error and the $\boldsymbol{v}_k$ intervals are based on 10 dB signal-to-noise ratio. In the case of SMF algorithm, the shape matrices of ellipsoidal sets for $\boldsymbol{w}_k$ and $\boldsymbol{v}_k$ have been estimated using the interval bounds as described in [14]. We also compare the performance of the SMF with the conventional EKF [20]. In the case of EKF, the corresponding noise co-variance matrices have been derived by assuming that above intervals correspond to four standard deviations. In simulations, which have been carried out in Matlab, a time step of 1 ms and a measurement interval of 10 ms have been used. These values were chosen based on the assumption that the terminal voltage and angle at the machine bus are available at every 0.01 s, which corresponds to a PMU rate of 100 samples/s.

Table 2: Normalized time-averaged MSE during the two faults.

State	Fault 1		Fault 2	
	EKF (10^{-6})	SMF (10^{-6})	EKF (10^{-5})	SMF (10^{-5})
e_{δ_k}	0.1967	0.1968	0.0641	0.0396
$e_{\Delta\omega_k}$	0.0003	0.0007	0.0001	0.0001
$e_{\psi_{fd_k}}$	0.2889	0.3382	0.0137	0.0190
$e_{\psi_{1d_k}}$	0.3648	0.4084	0.0432	0.0446
$e_{\psi_{1q_k}}$	0.2631	0.2049	0.1029	0.0525
$e_{\psi_{2q_k}}$	0.5855	0.5516	0.2416	0.2011

In order to test the SMF algorithm, we carried out the following experiment. First, a bus fault is applied at the infinite bus of the SMIB system operating in steady state. The fault is then cleared and the system is allowed to return back to the steady state. Next a balanced fault is applied at the mid point of Line 2. This experiment allows us to observe the ability of the SMF algorithm to track the system state under steady-state conditions without requiring any correction-step updates (thus, for example, ignoring PMU measurements), while maintaining accurate tracking during a fault using frequent correction steps. The estimated states and the exact system states before, during, and after the two fault events are shown in Fig. 2. Also shown are the states estimated by the conventional EKF algorithm. In this experiment as well as in other experiments, it was observed that the tracking performance of SMF is very similar to that of EKF. Comparison of the normalized time-averaged MSE during fault conditions for the algorithms are presented in Table 2.
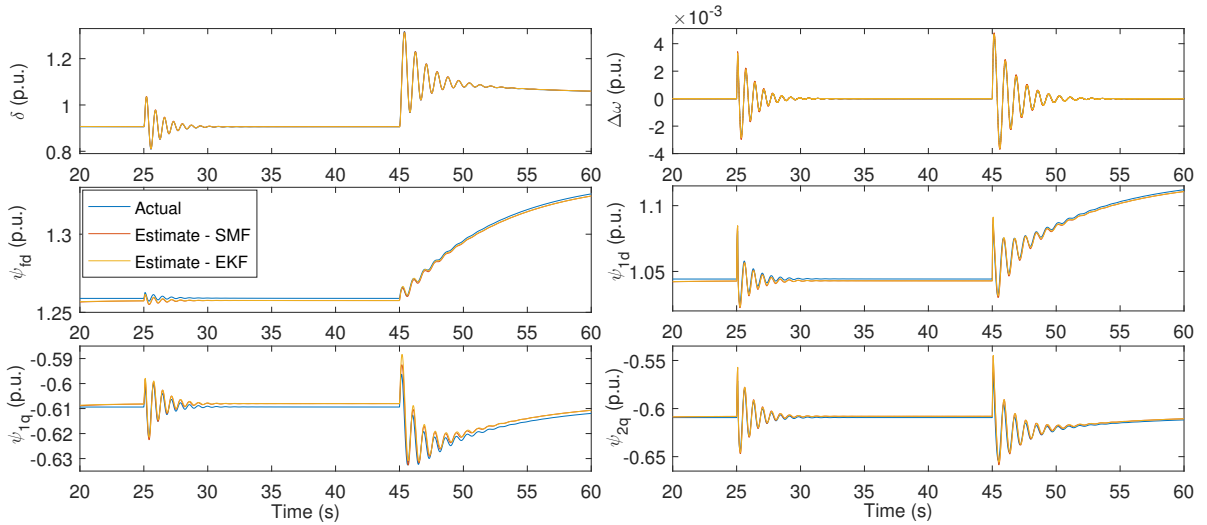

Figure 2: Comparison of state estimates.

It has been observed that the SMF algorithm carried out the complete correction step on the average only 31.1% of the time during 1st fault and on the average only 42.2% of the time during 2nd fault. This indicates that more than 50% of the time the predicted state needs no updates even during a disturbance. However, the estimation result obtained from the SMF algorithm is comparable to that of EKF. Fig 3 (A) shows the normalized average correction steps variation over the time. Also it has been observed that after initialization, the SMF algorithm performs the complete correction step until the steady-state is reached, after which no correction steps are required until a disturbance occurs. This indicates the applicability of the SMF for event-triggered state estimation in the context of power systems.

In order to investigate the impact of inevitable modeling errors on the performance of the SMF, $\pm p\%$ error has been introduced to X_d'', and X_q'' in the equations used in state estimator. Even a parameter error of $\pm 1\%$ has a significant impact on the normalized time averaged MSE of estimates which is in the range of 10^{-2}. Due to the introduced modeling error, the SMF state estimator takes more time to converge and also results in more than 10% increase in the normalized average correction steps during the disturbance
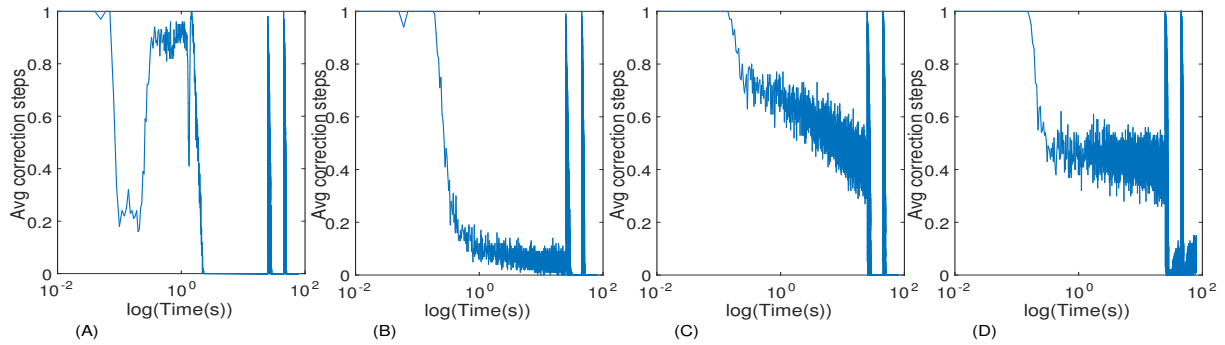
Figure 3: Normalized average of correction steps as a function of time.

as shown in Fig 3 (B).

Further, if the modeling error is above $\pm 5\%$ the advantage of event-triggered state estimation is lost. Fig 3 (C) and (D) shows the variation of the normalized average correction steps when the modeling error is $\pm 5\%$ and $\pm 10\%$ respectively. The normalized time averaged MSE of estimates will also increase making the estimation obsolete in both the SMF and the EKF algorithms.

4   CONCLUSION

It has been shown that the SMF algorithm with a selective correction step does not create any adverse effect on state estimation in comparison with the KF algorithm and the complete correction step calculation was required only during a small fraction of time. The SMF algorithm can be implemented at the local estimators in the MASE context. Then in the event of a state change, the SMF algorithm can identify it based on its data selective capability. This can be used as a criterion to send the state information to the centralized estimator for further processing. Consequently, this will significantly reduce the communication overhead in power systems with PMUs. However, it has been demonstrated that the modeling error will seriously degrade the estimation accuracy. This is an issue that has to be addressed in future work.

BIBLIOGRAPHY

[1] J. Zhao, A. Gómez-Expósito, M. Netto, L. Mili, A. Abur, V. Terzija, I. Kamwa, B. Pal, A. K. Singh, J. Qi, *et al.*, "Power system dynamic state estimation: Motivations, definitions, methodologies, and future work," *IEEE Transactions on Power Systems*, vol. 34, no. 4, pp. 3188–3198, 2019.

[2] Y.-F. Huang, S. Werner, J. Huang, N. Kashyap, and V. Gupta, "State estimation in electric power grids: meeting new challenges presented by the requirements of the future grid," *IEEE Signal Processing Magazine*, vol. 29, pp. 33–43, Sept. 2012.

[3] S. Kapoor, S. Gollamudi, S. Nagaraj, and Y. Huang, "Tracking of time-varying parameters using optimal bounding ellipsoid algorithms," in *Proceedings of the Annual Allerton Conference on Communication Control and Computing*, vol. 34, pp. 392–401, Citeseer, 1996.

[4] P. Kundur, N. J. Balu, and M. G. Lauby, *Power system stability and control*, vol. 7. McGraw-hill New York, 1994.

[5] A. Abur and A. G. Exposito, *Power System State Estimation: Theory and Implementation*, vol. 24 of *Power Engineering (Willis)*. CRC Press, Mar. 2004.

[6] A. Monticelli, "Electric power system state estimation," *Proceedings of the IEEE*, vol. 88, pp. 262–282, Feb. 2000.

[7] I. S. Association *et al.*, "Ieee standard for synchrophasor measurements for power systems," *IEEE Std C*, vol. 37, pp. 1–61, 2011.

[8] L. Zhao and A. Abur, "Multi area state estimation using synchronized phasor measurements," *IEEE Transactions on Power Systems*, vol. 20, no. 2, pp. 611–617, 2005.

[9] F. Schweppe, "Recursive state estimation: unknown but bounded errors and system inputs," *IEEE Trans. Autom. Control.*, vol. AC-13, pp. 22–28, Feb. 1968.

[10] D. Bertsekas and I. Rhodes, "Recursive state estimation for a set-membership description of uncertainty," *IEEE Trans. Automat. Contr.*, vol. 16, pp. 117–128, Apr. 1971.

[11] F. Schlaepfer and F. Schweppe, "Continuous-time state estimation under disturbances bounded by convex sets," *IEEE Trans. Autom. Control.*, vol. 17, pp. 197 – 205, Apr. 1972.

[12] E. Fogel and Y. Huang, "On the value of information in system identification—bounded noise case," *Automatica*, vol. 18, pp. 229–238, Mar. 1982.

[13] Y. Huang, "A recursive estimation algorithm using selective updating for spectral analysis and adaptive signal processing," *IEEE Trans. Acoust., Speech, Signal Process.*, vol. 34, pp. 1331–1334, Oct. 1986.

[14] F. L. Chernousko, *State Estimation for Dynamic Systems*. CRC Press, Inc.: Boca Raton,FL, 1994.

[15] J. Zhao, G. Zhang, K. Das, G. N. Korres, N. M. Manousakis, A. K. Sinha, and Z. He, "Power system real-Time monitoring by using PMU-based robust state estimation method," *IEEE Transactions on Smart Grid*, vol. 7, pp. 300–309, Jan. 2016.

[16] S. Dasgupta and Yih-Fang Huang, "Asymptotically convergent modified recursive least-squares with data-dependent updating and forgetting factor for systems with bounded noise," *IEEE Trans. Inf. Theory.*, vol. 33, pp. 383–392, May 1987.

[17] C. Durieu, . Walter, and B. Polyak, "Multi-input multi-output ellipsoidal state bounding," *Journal of Optimization Theory and Applications*, vol. 111, pp. 273–303, Nov. 2001.

[18] Y. Liu, Y. Zhao, and F. Wu, "Ellipsoidal state-bounding-based set-membership estimation for linear system with unknown-but-bounded disturbances," *IET Control Theory & Applications*, vol. 10, no. 4, pp. 431–442, 2016.

[19] Y. Liu, Y. Zhao, and F. Wu, "Extended ellipsoidal outer-bounding set-membership estimation for nonlinear discrete-time systems with unknown-but-bounded disturbances," *Discrete Dynamics in Nature and Society*, vol. 2016, 2016.

[20] S. G. Mohinder and P. A. Angus, *Kalman Filtering: Theory and Practice Using MATLAB*. Wiley, 2015.